JOURNAL OF MATERIALS SCIENCE: MATERIALS IN MEDICINE, 7 (1996) 567–578

Electrocapillary properties of tryptophan

J. B. CRAIG*, C. MACKAY
Department of Chemistry, University of Aberdeen, Meston Walk, Old Aberdeen, AB9 2UE, UK

This paper describes the electrocapillary properties of the amino-acid tryptophan in 0.165 M sodium chloride over the temperature range 20–40 °C. Surface excess concentrations, as functions of electrical potential and charge density of the mercury surface, together with Esin and Markov and other differential cross-coefficients, show that the Volmer adsorption equation fits the experimental data very well, and that adsorption is congruent to both potential and charge density, but that such congruency is imperfect. The minimum surface area occupied by the adsorbed molecule is commensurate with the indole ring lying flat on the mercury surface. At zero and positive charge densities, the flat configuration permits maximum π-electron interaction with the aromatic moiety and at the same time permits freedom of rotation around the C_α–C_β bond. At progressively more negative charge densities, the electrical repulsion between the mercury and the π-electron structure presents an unfavourable situation for adsorption. The zwitter-ion moiety appears to play only a minor role in adsorption. It is proposed that one reason why some artificial prostheses surfaces are incompatible with blood and tissue components is that in biological media such surfaces may adopt a zero or positive charge density attracting the aromatic moieties, such as tryptophan, of tissue and blood protein molecules: the adsorption process would be the initial step in a cascade series of detrimental reactions. The surface electrochemical properties of prostheses surfaces in biological media should therefore be seriously considered when formulating new materials.

1. Introduction

A prosthesis coming into contact with either body tissue or blood undergoes numerous interfacial reactions, the nature of each being exceedingly complex. In general terms, the timescale for these reactions can range from seconds, in the case of blood, to years, in the case of tissues. It is widely accepted that the initial event in the contact between prosthesis and blood is the adsorption by the prosthesis of a layer of plasma protein [1], the structure and composition of which determines the pathway of subsequent deleterious reactions [2–4]. Hence a detailed study of the initial event should provide a greater insight into the problems of biocompatibility.

The main components of the adsorbed layer are fibrinogen, γ-globulins, and albumins. Surfaces which preferentially adsorb fibrinogen and γ-globulins are, in relative terms, more thrombogenic than those that adsorb albumins. Although fibrinogen and the γ-globulins differ in many ways from the albumins, one obvious difference is in their percentage composition (2.86, 3.29, and 0.19, respectively) of the amino-acid fragment tryptophan. The possibility that large blood protein molecules are anchored to thrombogenic surfaces via their tryptophan moieties, should therefore be investigated.

The ever-increasing use of electrodes as diagnostic and control devices shows that the electrical nature of the prosthesis surface plays an important role in stimulating blood and tissue response: this observation led us to consider that one of the principal causes of biocompatibility may be electrostatic in origin. Duic [5] believes that accumulated evidence indicates that thrombosis occurs as a result of interfacial electrochemical reactions with positively-charged surfaces initiating, and negatively-charged surfaces inhibiting, thrombosis. Mattison [6] has shown that fibrinogen adsorption is enhanced at positive potentials. The observation that streaming and zeta potentials of blood vessels *in vitro* were small and negative [7], and that the zeta potential of the intima *in vivo* is also negative [8], would indicate that a negatively-charged surface is one condition for compatibility. Polymers of differing composition but having the same zeta potential show a great variation in compatibility, but, in general, those bearing the most negative potential were the most compatible [9], while those with positive potentials were the most thrombogenic [10]. These observations did not show clearly (a) the origin of the potential on the prosthesis surface, (b) whether the driving force for the interfacial reaction was potential, field, or charge density, and (c) the mechanisms by which globular proteins were adsorbed.

It was felt that detailed studies on simpler model systems were required. Mercury was chosen as a model for the prosthesis because (a) the electrical

0957–4530

charge can be taken as uniformly spread over the surface, (b) it can be obtained in high purity, (c) mercury/solution interfacial tensions can be measured easily [11], and (d) the surface charge can be controlled. Mercury is unsuitable for adsorption studies of electroactive biomedical species. Amino acids in aqueous saline solutions were used as models for blood and tissue regimes with tryptophan as the first amino acid for study.

2. Theory

The thermodynamics of the electrical double layer, based on the Gibbs adsorption equation, Equation 1, were applied to charged interfaces by Grahame [12], and to solutions of salts and neutral non-dissociating components by Parsons [13].

$$d\gamma = -q\,dE - \left(\frac{q}{z_j F}\right)d\mu_j - \sum_i \Gamma_i\,d\mu_i \qquad (1)$$

where γ = interfacial tension, q = charge density on the mercury surface, E = electrical potential of the mercury with respect to a reference electrode reversible to ion j (Cl^- here), μ = (electro)chemical potential, i = ion, polar, or neutral species under consideration, Γ = surface excess concentration. At constant temperature, pressure, and solution composition, the Gibbs equation reduces to the Lippmann equation (equation 2a), and at constant temperature, pressure, and electrical potential, to Equation 2b:

$$\left(\frac{d\gamma}{dE}\right)_{\mu_j,\mu_i} = -q = q_s \qquad (2a)$$

$$(d\gamma)_{E,\mu_{Cl^-}} = -\Gamma_w\,d\mu_w - \Gamma_o\,d\mu_o \qquad (2b)$$

where q_s = charge density on the solution side of the interface, and subscripts w and o signify the water and neutral amino acid components, respectively. An expression analogous to Equation 2 employing the surface pressure (π) instead of interfacial tension is obtained by substituting ($d\gamma$) with -($d\pi$). We adopt the Guggenheim convention [14] for the definition of the relative surface excess concentration of the amino acid, and further, assume that for dilute solutions the activity coefficient of the amino acid is unity, hence

$$-\frac{1}{RT}\left(\frac{d\gamma}{d\ln c_o}\right)_{E,\mu_{Cl^-},\Gamma_w = 0} = \frac{1}{RT}\left(\frac{d\pi}{d\ln c_o}\right)_{E,\mu_{Cl^-},\Gamma_w=0} = \Gamma_o \qquad (3)$$

Equation 3 is based on the assumption that the correct electrical variable is potential, but when the controlling variable is charge density, Parsons [15] has shown that the interfacial tension should be replaced with an auxiliary function ξ, defined as $\xi = \gamma + qE$, with the analogue corresponding to π being ϕ. Hence,

$$-\frac{1}{RT}\left(\frac{d\xi}{d\ln c_o}\right)_{q,\mu_{Cl^-},\Gamma_w=0} = \frac{1}{RT}\left(\frac{d\phi}{d\ln c_o}\right)_{q,\mu_{Cl^-},\Gamma_w=0} = \Gamma_o \qquad (4)$$

The forms of the Gibbs adsorption equation are total differentials and therefore continuous derivatives of the interfacial tension of all orders. The second-order partial cross derivatives of Equation 1 are of particular interest, thus

$$\frac{1}{RT}\left(\frac{dq}{d\ln c_o}\right)_{E,\mu_{Cl^-}} = \left(\frac{d\Gamma}{dE}\right)_{\mu_{Cl^-},\mu_o} \qquad (5)$$

which implies that if the charge density of mercury varies with the concentration of organic solute, at constant potential, then the surface excess concentration of that solute is a function of potential. Similarly, the relationship

$$\frac{1}{RT}\left(\frac{dE}{d\ln c_o}\right)_{q,\mu_{Cl^-}} = -\left(\frac{d\Gamma}{dq}\right)_{\mu_{Cl^-}} \qquad (6)$$

can be obtained which implies that if the potential varies with concentration, at constant charge density, then the surface excess concentration is a function of charge density. The term on the left-hand side of Equation 6 is the Esin and Markov coefficient, and Equations 5 and 6 are useful for checking experimental accuracy.

If a neutral organic solute is strongly adsorbed at the electrical double layer, the surface excess concentration differs little from the surface concentration, so that for dilute solutions

$$\mu^{o,s} + RT\ln\left(\frac{\Gamma}{\Gamma^o}\right) = \mu^{o,b} + RT\ln\left(\frac{c}{c^o}\right) \qquad (7)$$

where the superscripts o, s, and b signify the standard state, surface phase, and bulk phase, respectively [16]: the subscript o has been omitted for clarity. The standard free energy of adsorption, ΔG^o, may be defined as

$$\Delta G^o = \mu^{o,s} - \mu^{o,b} \qquad (8)$$

and letting

$$\beta = e^{-(\Delta G^o/RT)} \qquad (9)$$

gives

$$\Gamma = \beta c \qquad (10)$$

Equation 10 is the general form of an adsorption isotherm: it expresses the surface concentration as a function of the bulk concentration and the electrical state of the system, which is included in the term β. At constant electrical variable, the surface pressures, π and ϕ, are related to the surface concentration through an equation of state, which corresponds to a definite physical model of the adsorbed layer on the mercury surface. Parsons [17, 18], following the work of Everett [19], has examined the form of several possible equations of state for the adsorbed layer and has derived the corresponding isotherms.

The standard free energy may be split formally into a chemical term, ΔG^o_{chem}, and an electrical term, though this is strictly correct when the charge density is zero. ΔG^o_{chem} describes the energy terms involved in taking the adsorbate from the bulk solution to the surface with the concommitant transfer of the adsorbed solvent and other solutes in the opposite direction. It involves many types of particle–particle interactions,

and is clearly a complex quantity on which to construct a molecular model. The electrical term reflects the metal–solute interactions only and Parsons [20] has suggested a semi-empirical equation in terms of an expanding series of the form

$$\Delta G^{\circ} = \Delta G^{\circ}_{\text{chem}} + aE + bE^2 \qquad (11)$$

The linear term arises from strong electrostatic interactions between the metal electrode and adsorbed ion or permanent dipole. The quadratic term represents the behaviour normally found in the adsorption of a neutral species, and is a property of the polarizability and thickness of both adsorbate and solvent monolayers, as shown by Frumkin [21].

When inspecting a set of π versus $\ln c$ curves, it may be seen that they have the same shape, but different position, and so may be superimposed on a common curve by lateral shifts along the $\ln c$ axis. This condition is known as congruence and it implies that the form and constants of the equation of state of the adsorbed film are independent of the electrical variable which has been held constant in the calculation of surface pressures, and further, that the free energy of adsorption at zero coverage is independent of the electrical variable. Dutkiewitz [22] found little difference in the adsorption isotherms using either variable: the isotherms were congruent to both electrical variables or to none at all, though Frumkin [23] has disputed this. Trasatti [24] has presented data which are not congruent to either variable. Congruency is therefore a difficult issue to clarify, and de Battisti [25] has suggested that the best course would be to analyse the adsorption of a neutral species at constant potential and at constant charge density to establish if, irrespective of any model, consistent results are found by the two procedures.

3. Experimental procedures

3.1. Materials

Sodium chloride and potassium chloride, Analar grade (BDH), were dried before use; L-tryptophan, chromatographically homogeneous (BDH), was used as received; water was double distilled in a quartz flask; mercury was washed with dilute nitric acid, rinsed with distilled water, dried, filtered, and triple-distilled under high vacuum.

3.2. Apparatus and procedure

This has been described in a previous paper [11]. Five temperatures were used, 293, 298, 303, 308, and 313 K. The base solution for all tryptophan solutions was 0.165 M sodium chloride. The tryptophan solution concentrations were W0 = 0 M, W1 = 9.790×10^{-5} M, W2 = 1.567×10^{-4} M, W3 = 2.938×10^{-4} M, W4 = 3.868×10^{-4} M, W5 = 6.027×10^{-4} M, W6 = 9.989×10^{-4} M, W7 = 1.004×10^{-3} M, W8 = 2.997×10^{-3} M, W9 = 9.989×10^{-3} M, W10 = 2.998×10^{-2} M. All potentials were measured with respect to a 0.1 M KCl/calomel electrode but quoted with respect to the standard hydrogen electrode (SHE).

4. Results

Electrical potential as the control variable. The electrocaplillary curves, γ versus E, of saline tryptophan were all smoothly parabolic in form and fitted well to 10th-order Chebychev polynomials, and showed γ decreasing with increasing concentration and temperature. The Lippmann curves, q versus E, showed that the point of zero charge (pzc) moved slightly to more negative potentials with increasing concentration, and that the q/E relationship becomes more sigmoidal indicating a minimum in the differential capacitance in the region of the pzc.

The curves of π versus E at constant composition, and at 298 K, shown in Fig. 1a are asymmetrical showing tryptophan to be more surface active at more positive potentials. π increased with increasing concentration and decreasing temperature. Each of 27 (π versus $\ln c)_{E,T}$ was shifted to give a composite curve for each temperature, as shown in Fig. 2a, with the heavy line representing the overall, best-fit, Chebychev polynomial and the (underlying) broken line representing the Volmer adsorption isotherm (discussed later): the agreement between each pair of lines is excellent at $\pi > 5\ \text{mN m}^{-1}$. (The choice of the reference curve, about which $\ln c$ shifts were made, was quite arbitrary, which accounts for both positive and negative values of $\Delta \ln c$, discussed later.) No such agreement was obtained with either the Henry, Langmuir, Frumkin, Temkin, or virial equation of state and corresonding adsorption isotherms: only the Volmer isotherm gave an excellent fit to the experimental data and all values of Γ used in subsequent calculations are based on this isotherm.

On the assumption that the activity coefficient of tryptophan in each solution was unity, the Volmer isotherm takes the form

$$\beta c = \pi e^{v\pi/RT} \qquad (12)$$

The values of the Volmer coefficient, v, are given in the first part of Table I.

$\Delta \ln c$ is related to the changes in the free energy of adsorption, i.e.

$$\Delta \ln c = -\Delta \ln \beta = \frac{\Delta(\Delta G^{\circ})}{RT} \qquad (13)$$

and since ΔG° is obtained from $\ln \beta$ of a reference curve, the relationship between the free energy of adsorption and potential can be obtained, and is shown in Fig. 3a. When the data are inserted into Equation 11, the coefficient of the linear term is very small, which implies that the amino-acid dipole plays little part in the adsorption process. The data fitted well a parabolic equation of the form

$$\Delta \ln c = -\Delta \ln \beta = (\text{constant}) + \tfrac{1}{2} g(E - E_{\text{m}})^2 \qquad (14)$$

where E_{m} is the potential at which $\Delta G^{\circ} = \Delta G^{\circ}_{\text{chem}}$. The theories of Butler [26] and Frumkin [27] are based on the assumption that a quadratic function is adequate to represent the variation of the standard free energy with the electric field, and this form of expression has also been used by Baugh [28]. Although each $\Delta \ln c$

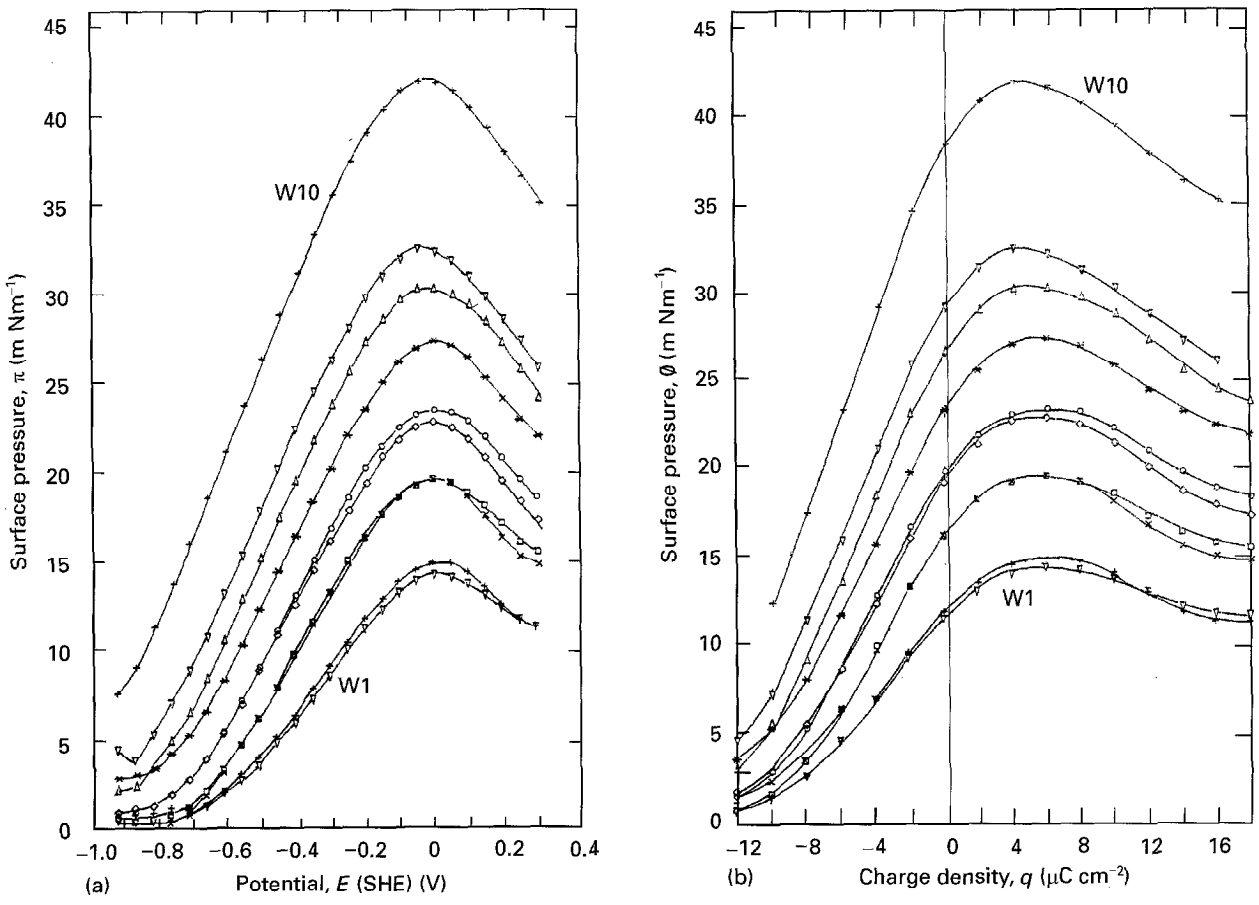

Figure 1 (a) Surface pressure, π, versus electrode potential, E. (b) Surface pressure, ϕ, versus charge density on the mercury surface, q. $T = 298$ K. ▽ w1, + w2, × w3, □ w4, ◇ w5, ○ w6, * w7, △ w8, ▽ w9, + w10.

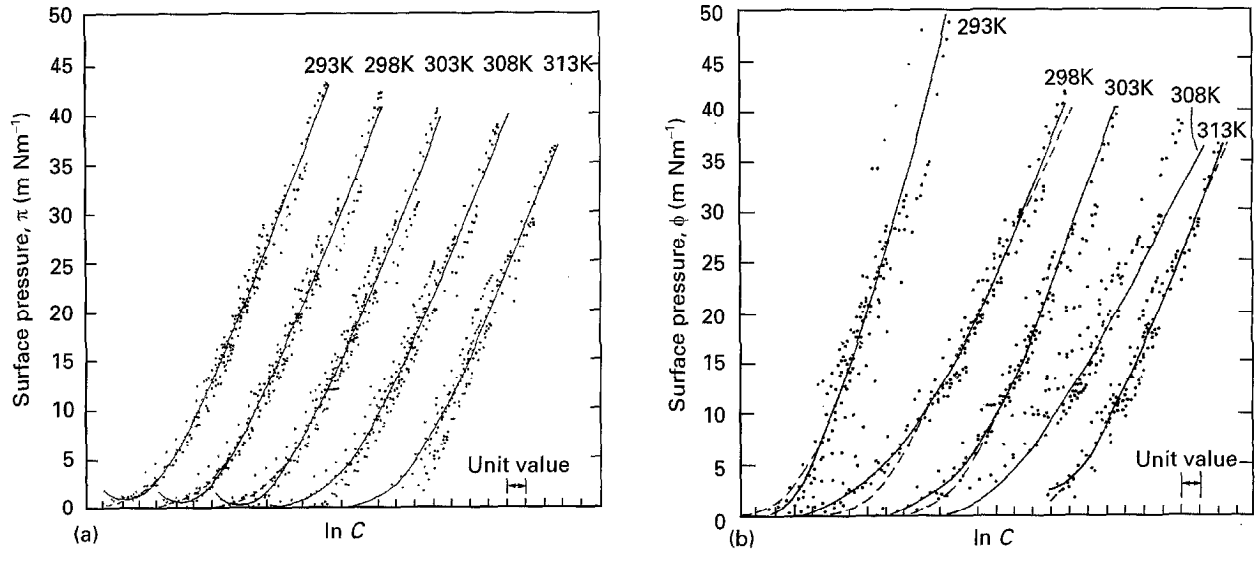

Figure 2 Composite curves of (a) surface pressure π, and (b) surface pressure ϕ, versus the natural logarithm of the concentration of tryptophan, $\ln c$. Heavy line denotes Chebychev polynomial; broken line (underneath) denotes the Volmer adsorption isotherm.

versus $(E - E_m)^2$ curve can be represented well by a second-order expression, it is obvious from Fig. 3a that the curves are not symmetrical, and hence would be better represented by two equations, one for the 'anodic', and one for the 'cathodic', branch. The pairs of g-values are given in Table II.

Charge density as the control variable. The surface pressure curves, ϕ versus q, Fig. 1b, show clearly that the maximum adsorption of tryptophan occurs at $+6 > q > +4\ \mu C\,cm^{-2}$. The curves are skew implying that the modes of adsorption on either side of the pzc differ. The adsorbed tryptophan is behaving neither as a simple neutral, nor as an ionic, species, but principally as an aromatic species with strong π-electron interaction when the mercury is positively charged. The (ϕ versus $\ln c)_q$, curves are similar to corresponding (π versus $\ln c$) ones in Fig. 2a, so in a similar manner, they were shifted along the $\ln c$ axis to obtain the set of composite curves shown in Fig. 2b: the reference curve was that for $q = 8\ \mu C\,cm^{-2}$. The heavy line represents

TABLE I Volmer adsorption coefficients v is given here in terms of A_{min}, the minimum area occupied per molecule, Equation 26. Correlation coefficients of $\ln(c/\pi)$ versus π/RT, and $\ln(c/\phi)$ versus ϕ/RT, respecively, are shown in parentheses. (The ϕ data contain a first-derivative term and hence are inherently less precise.)

Control variable	Potential	Charge density
T (K)	(v/nm^2)	(v/nm^2)
293	0.700 (0.9999)	0.480 (0.9999)
298	0.737 (0.9999)	0.867 (0.9986)
303	0.758 (0.9999)	0.662 (0.9997)
308	0.777 (0.9999)	1.120 (0.9999)
313	0.736 (0.9999)	0.794 (0.9999)

the best-fit 4th-order Chebychev polynomial, while the broken line represents the Volmer adsorption isotherm. The Volmer coefficients are given in the second part of Table I. The shifts of the experimental curves $(\Delta \ln c)_q$, and the corresponding ΔG°, are shown in Fig. 3b as a function of charge density. The curves are quadratic in form, so the charge analogue of Equation 14,

$$\Delta \ln c = -\Delta \ln \beta = (\text{constant}) + \tfrac{1}{2}g'(q - q_m)^2 \quad (15)$$

was used to confirm this: the values of g' are given in Table III.

The Esin and Markov plots, q_E versus $\ln c$ and E_q versus $\ln c$, Fig. 4, are linear but the correlation coefficients for the extreme anodic and cathodic portions are less good. The corresponding Esin and Markov coefficients, $(dq/d\ln c)_E$ and $(dE/d\ln c)_q$, are shown as a function of E and q, respectively, in Fig. 5. Differentiation of Equation 5 with respect to potential gives

$$\frac{d^2q}{d\ln c \cdot dE} = RT\left(\frac{d^2\Gamma}{dE^2}\right) \quad (16)$$

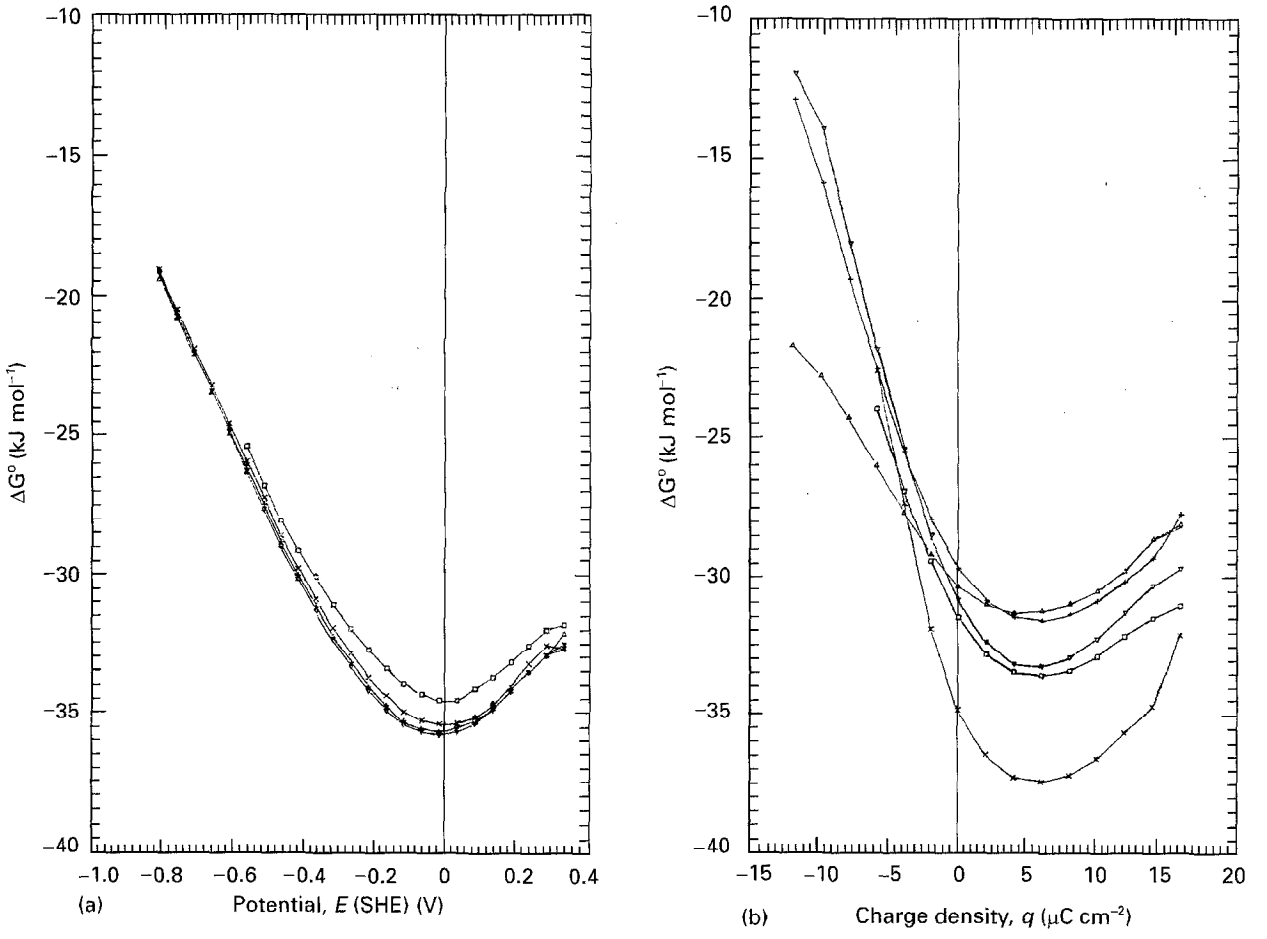

Figure 3 Free energy of adsorption, ΔG°, versus (a) electrode potential, and (b) charge density on the mercury surface. $\triangle$ = 293 K, ∇ = 298 K, + = 303 K, × = 308 K, □ = 313 K.

TABLE II Values of the term g derived from Equations 14 and 22 with the corresponding correlation coefficients given in parentheses

T (K)	g (V^{-2})			
	Derived from Equation 14		Derived from Equation 22 and Fig. 8a	
	Anodic potentials	Cathodic potentials	Anodic potentials	Cathodic potentials
293	11.51 (0.992)	12.00 (0.997)	11.86 (0.969)	9.08 (0.997)
298	11.28 (0.982)	12.00 (0.997)	11.39 (0.943)	9.19 (0.950)
303	10.41 (0.976)	11.80 (0.996)	12.25 (0.949)	8.59 (0.947)
308	10.07 (0.958)	11.42 (0.996)	11.69 (0.921)	8.26 (0.956)
313	9.08 (0.975)	11.40 (0.996)	7.42 (0.819)	8.21 (0.979)

TABLE III Values of the term g', derived from Equations 15 and 23, with the corresponding correlation coefficients given in parentheses

T (K)	g' $(\mu C\,cm^{-2})^{-2}$			
	Derived from Equation 15		Derived from Equation 23 and Fig. 8b	
	Anodic potentials	Cathodic potentials	Anodic potentials	Cathodic potentials
293	0.022 (0.997)	0.047 (0.999)	0.015 (0.870)	0.081 (0.980)
298	0.029 (0.977)	0.061 (0.997)	0.031 (0.808)	0.173 (0.983)
303	0.030 (0.998)	0.046 (0.998)	0.019 (0.815)	0.108 (0.987)
308	0.040 (0.992)	0.068 (0.996)	0.041 (0.871)	0.211 (0.938)
313	0.020 (0.975)	0.050 (0.998)	0.021 (0.835)	0.103 (0.943)

Fig. 5 shows that $(dq/d\ln c)_E$ is a linear function of E over the potential range $0.0 > E > -0.7$ V, therefore $\Gamma(\pi)$ should be a quadratic function of E over the same region, but it is obvious from the $\Gamma(\pi)$ versus E plots, Fig. 6a, that there are differing anodic and cathodic functions, i.e.

$$\Gamma(\pi) = \Gamma^m - \tfrac{1}{2}d_a(E-E^m)^2; \quad \frac{d^2\Gamma}{dE^2} = -d_a \quad \text{at } E > E^m \qquad (17a)$$

$$\Gamma(\pi) = \Gamma^m - \tfrac{1}{2}d_c(E-E^m)^2; \quad \frac{d^2\Gamma}{dE^2} = -d_c \quad \text{at } E < E^m \qquad (17b)$$

where E^m is the potential at which Γ is a maximum, Γ^m. A regression analysis of $\Gamma(\pi)$ versus $(E-E^m)^2$ is given in Table IV, and a comparison of RTd_a and RTd_c is made with the Esin and Markov coefficient with potential. It can be seen that though $\Gamma(\pi)$ is a fairly good quadratic function of E, indicating a high degree of congruency with potential, RTd_a is significantly less than $-(d^2q/d\ln c \cdot dE)$.

The curves of $\Gamma(\phi)$ versus q in Fig. 6 show clearly that maximum adsorption occurs when the mercury is positively charged, between 4 and 6 $\mu C\,cm^{-2}$. If $\Gamma(\phi)$ is a quadratic function of q, then the coefficient for the anodic branch is significantly less than that for the corresponding cathodic branch. Differentiation of Equation 6 with respect to charge gives

$$\frac{d^2E}{d\ln c \cdot dq} = -RT\left(\frac{d^2\Gamma}{dq^2}\right) \qquad (18)$$

The Esin and Markov coefficient $(dE/d\ln c)_q$ is a linear function of q, Fig. 5b, in the cathodic branch ($-8 < q < +6\ \mu C\,cm^{-2}$), and approximately linear, but of differing slope, in the anodic branch ($+6 < q < +14\ \mu C\,cm^{-2}$). Therefore, $\Gamma(\phi)$ should be a quadratic function of q in both branches, i.e.

$$\Gamma(\phi) = \Gamma^m - \tfrac{1}{2}d'_a(q-q^m)^2; \quad \frac{d^2\Gamma}{dq^2} = d'_a \quad \text{at } q > q^m \qquad (19a)$$

$$\Gamma(\phi) = \Gamma^m - \tfrac{1}{2}d'_c(q-q^m)^2; \quad \frac{d^2\Gamma}{dq^2} = d'_c \quad \text{at } q < q^m \qquad (19b)$$

where d'_a and d'_c are the respective coefficients of the anodic and cathodic branches: q^m is the value of q when $\Gamma(\phi)$ is a maximum. The regression analysis of $\Gamma(\phi)$ against $(q-q^m)^2$ is given in Table IV, and comparisons of RTd'_a and RTd'_c are made with the values of the corresponding $(d^2E/d\ln c\,dq)$ terms: there is some measure of agreement between the two second-order coefficients.

In his work on solvent and molecular orientation, Conway [29] used the term $d(\Delta E)_q/d\Gamma$, i.e., the variation in shift of potential, at constant charge, with surface excess concentration but incorrectly called this term an Esin and Markov coefficient, though it is related to it through the equation of state. Our curves of E_q versus $\Gamma(\pi)$ are all linear, Fig. 7b.

We can introduce a term, analogous to Conway's, which relates the shift in charge density, at constant potential, with the surface excess concentration $\Gamma(\phi)$, i.e. $d(\Delta q)_E/d\Gamma$. Plots of q_E verus $\Gamma(\phi)$ shown in Fig. 7a are all linear. According to Parsons [30], if an isotherm is congruent to potential, then

$$q - q_{base} = RT\Gamma\frac{\partial\ln\beta}{\partial E} \qquad (20)$$

where q_{base} is the value of q in the base solution, and since the standard free energy has been shown to be a function of potential, then

$$\frac{\partial\ln\beta}{\partial E} = -g(E-E_m) \qquad (21)$$

hence

$$\left(\frac{\partial^2 q}{\partial\Gamma\,\partial E}\right) = -gRT \qquad (22)$$

Plots of $\partial q/\partial\Gamma)_E$ versus E, Fig. 8a, show some departure from linearity: the values of g obtained by linear regression over two regions are given in Table II for comparison with the values of g obtained with Equation 14.

Similarly, if the adsorption isotherm is congruent to charge density, then it can be shown that

$$\left(\frac{\partial^2 E}{\partial\Gamma\,\partial q}\right) = -g'RT \qquad (23)$$

The plot of $(\partial E/\partial\Gamma)_q$ versus q, Fig. 8b, is not linear overall, but approximately linear in the anodic and in the cathodic regions. The paired values of g' are shown in Table III for comparison with the values of g' obtained with Equation 15.

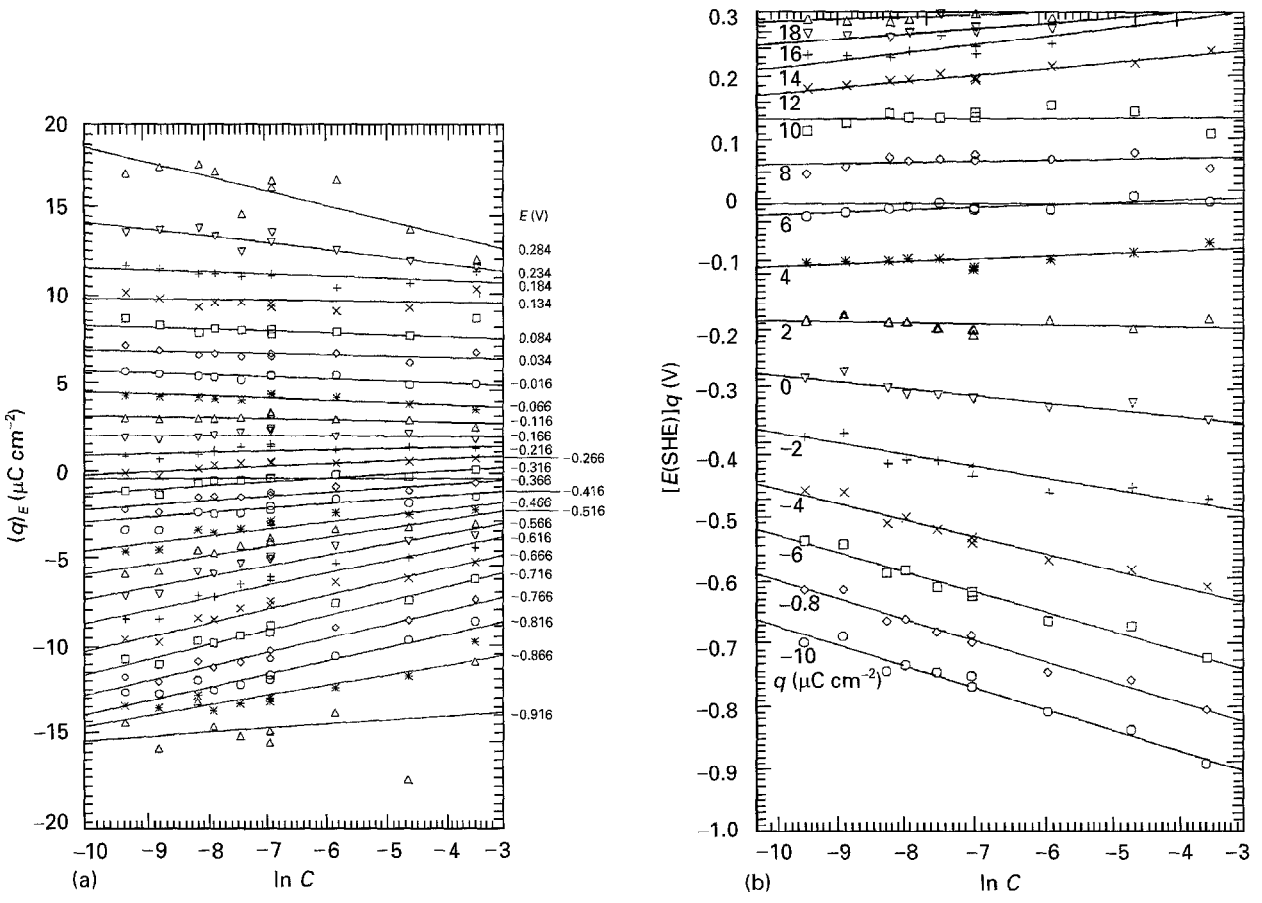

Figure 4 Esin and Markov plots: (a) q_E, and (b) E_q, respectively versus $\ln c$, at 298 K.

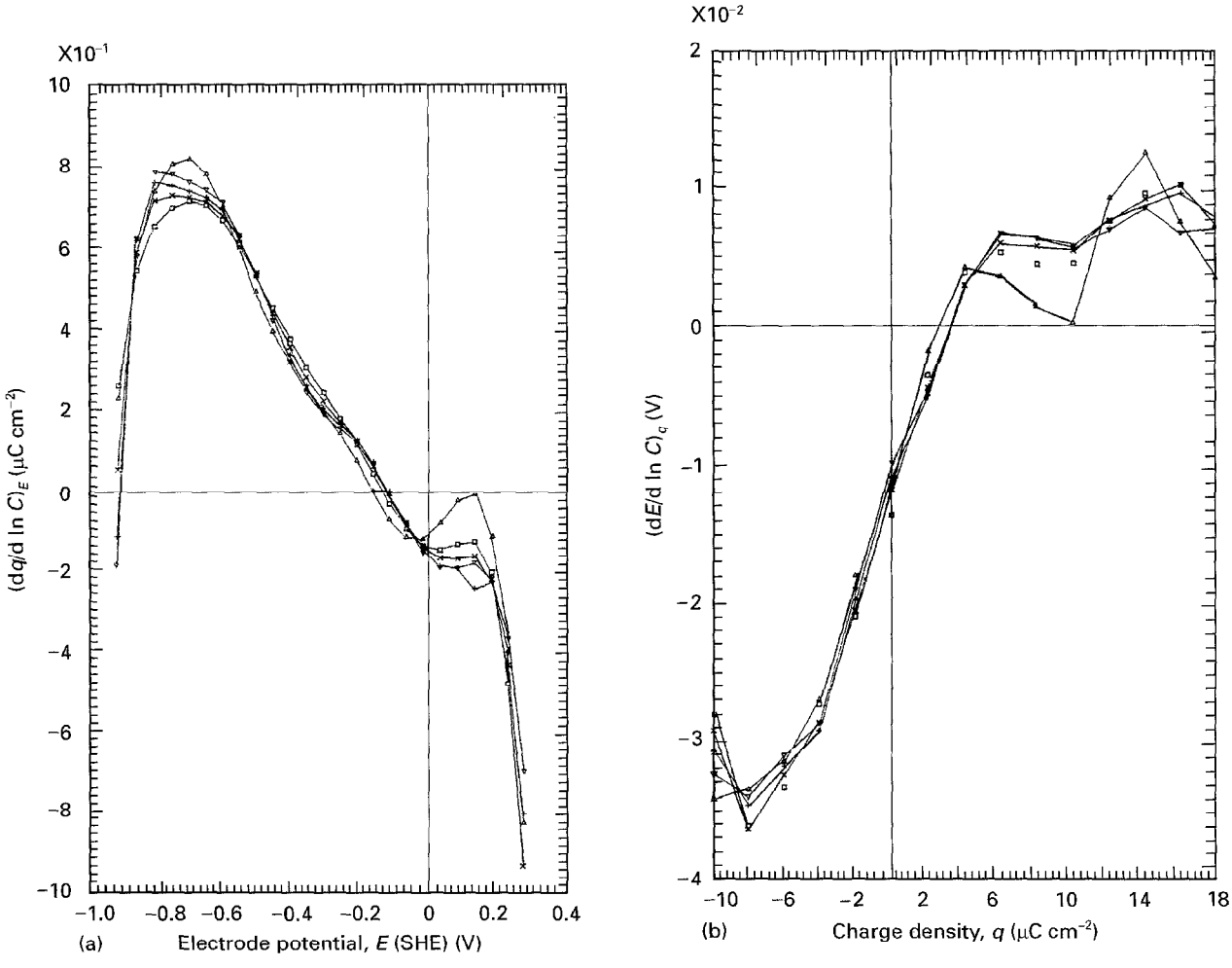

Figure 5 Esin and Markov coefficients (a) $(dq/d \ln c)_E$ versus potential E, and (b) $(dE/d \ln c)_q$ versus charge density q. Symbols as in Fig. 3.

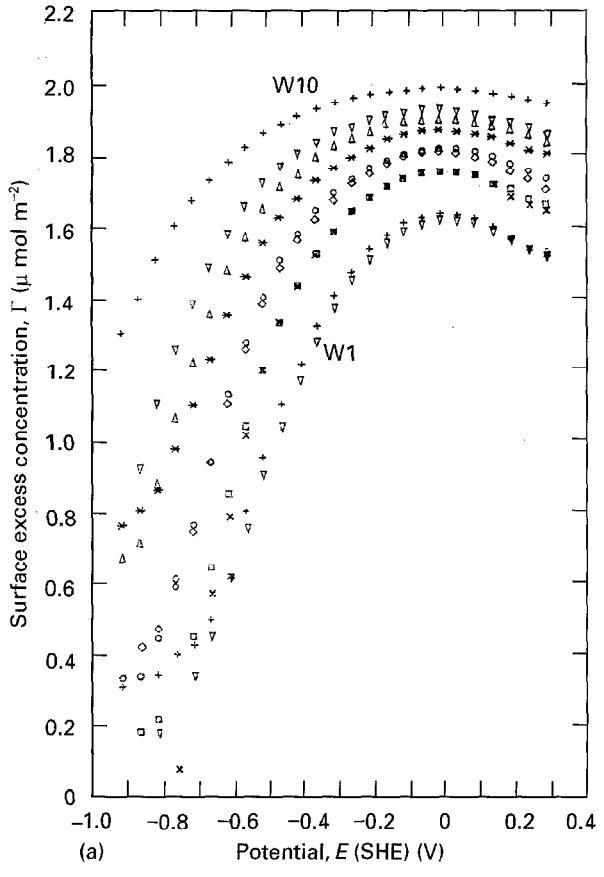

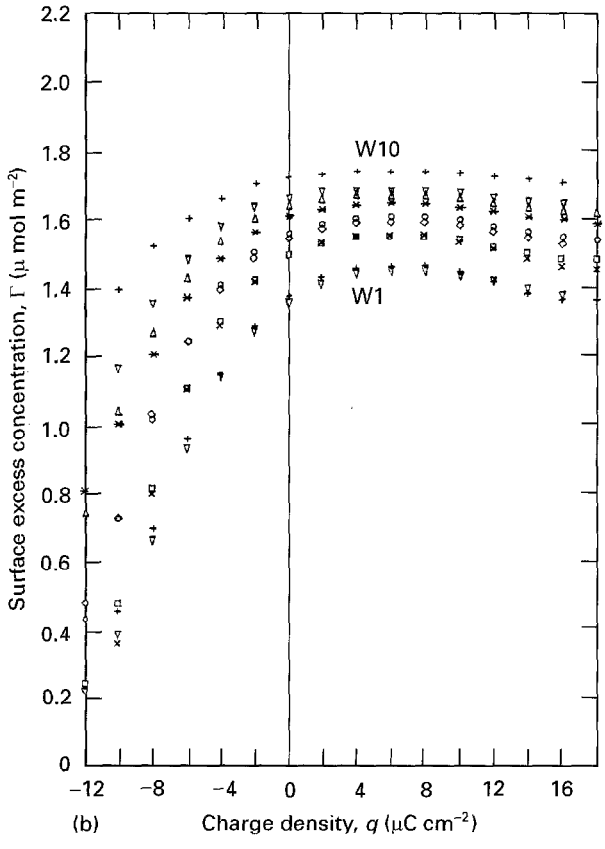

Figure 6 Surface excess concentration of tryptophan (a) $\Gamma(\pi)$ as a function of potential E, and (b) $\Gamma(\phi)$ as a function of charge density, q. Symbols as in Fig. 1.

The Volmer adsorption isotherm may be written in the form

$$\Gamma(\pi) = \left[RT\left(\frac{1}{\pi} + \frac{v}{RT}\right)\right]^{-1};$$

$$\Gamma(\phi) = \left[RT\left(\frac{1}{\phi} + \frac{v}{RT}\right)\right]^{-1} \quad (24)$$

From which it may be seen that at infinite surface pressure

$$v = [\Gamma^m]^{-1} \quad (25)$$

hence the minimum surface area occupied per molecule, A_{min} is

$$A_{min} = \frac{1}{N_A}\Gamma^m = \frac{v}{N_A} \quad (26)$$

where N_A is Avogadro's number. The pressure–area curves are shown in Fig. 9 and the A_{min} values are given in Table I: the values from the ϕ data are more scattered than those from the data because the former contains a first-derivative term and has inherent inaccuracies. A projection of the molecule of tryptophan lying flat on a surface shows that the area occupied is 0.766 nm^2, which is in agreement with the values given in Table I, thus confirming our belief that the molecule attains this configuration when adsorbed on a mercury surface.

5. Discussion

The configuration of tryptophan as a single isolated molecule has been obtained with a computer modeling package, and the corresponding Catalin-type space model is shown in Fig. 10. In aqueous solution, the configuration will be different because of the electrostatic and van der Waals interaction with surrounding solvent and solute molecules and the polarized mercury surface. Some of the tryptophan molecules will exist in the neutral state, some as zwitter-ions, the ratio of the two types depending on pH, ionic strength, and dielectric constant.

When mercury is positively charged, the strong attraction for the ten π-electrons of the aromatic rings will lead to the electron density on the mercury-side of the molecule being greater than that on the solution-side. An attempt has been made to show this on the space model, Fig. 10b, where the plane of the ring hydrogens, shown as a broken line, is above the mid-plane of the π-orbitals. The methylene hydrogens on the beta-carbon, C_β, are clear of the mercury surface allowing unhindered interaction between the π-electrons and the electron-deficient orbitals of the surface mercury atoms. In addition, the amino-acid group, whether ionic or not, is able to rotate unimpeded around the C_α–C_β bond.

When the mercury has zero charge, the attraction between the mercury will be of the van der Waal type only, and the plane of the ring hydrogens will approximate to the mid-plane of the π-orbitals, Fig. 10a. In this configuration, the tryptophan could still be lying flat, but the position is less favourable as the C_β-hydrogens would tend to tilt the indole ring, and rotation about the C_α–C_β bond would be inhibited to some extent: this would account for the fact that adsorption is not at its maximum value at the point of zero charge.

When the mercury is negatively charged, the plane of the ring hydrogens will be below the mid-plane of

TABLE IV (a) Regression analysis of $\Gamma(\pi, 293\,K)$ against $(E - E^m)^2$, Equations 17a, b: $E_m = -0.016$ V (SHE). Average values of $(d^2q/(d\ln c \cdot dE))$ obtained from Fig. 5a are given for comparison. (b) Regression analysis of $\Gamma(\phi, 293\,K)$ against $(q - q^m)^2$, Equations 19a, b: $q^m = 6\,\mu C\,cm^{-2}$. Average values of $(d^2E/(d\ln c \cdot dq))$ obtained from Fig. 5b are given for comparison. Correlation coefficients are given in parentheses

Solution	a	a	b	b
	d_a (10^{-6} mol m^{-2} V^{-2}) 'Anodic' branch ($0.334\,V > E > E^m$)	d_c (10^{-6} mol m^{-2} V^{-2}) 'Cathodic' branch ($E^m > E > -0.666$ V)	d'_a (10^{-4} mol m^2 C^{-2}) 'Anodic' branch ($14\,\mu C\,cm^{-2} > q > q^m$)	d_c (10^{-4} mol m^2 C^{-2}) 'Cathodic' branch ($q^m > q > -8\,\mu C\,cm^{-2}$)
W1	1.32 (0.998)	5.88 (1.000)	0.398 (0.988)	1.376 (0.998)
W2	4.48 (0.998)	6.10 (0.990)	0.580 (0.997)	1.375 (0.997)
W3	3.84 (1.000)	5.20 (0.992)	0.481 (0.992)	1.326 (0.991)
W4	3.53 (0.994)	4.74 (0.995)	0.429 (0.987)	1.227 (0.993)
W5	3.02 (1.000)	4.04 (0.992)	0.431 (0.999)	1.132 (0.990)
W6	2.85 (0.994)	3.84 (0.992)	0.327 (0.986)	1.103 (0.991)
W7	2.60 (0.999)	3.02 (0.994)	0.376 (0.999)	0.929 (0.992)
W8	1.86 (0.997)	2.42 (0.990)	0.288 (0.992)	0.836 (0.986)
W9	2.02 (0.984)	1.78 (0.963)	0.196 (0.999)	1.009 (0.995)
W10	0.78 (0.972)	1.20 (0.994)	0.120 (0.995)	0.277 (0.993)
	average $RT\,d_a = 0.68*10^{-2}$ J m^{-2} V^{-2} $-(d^2q/(d\ln c \cdot dE) = 1.30*10^{-2}$ J m^{-2} V^{-2}		average $RT\,d'_a = 0.0982$ J m^2 C^{-2} $-(d^2E/(d\ln c \cdot dq) = 0.0558$ J m^2 C^{-2}	
	average $RT\,d_c = 0.96*10^{-2}$ J m^{-2} V^{-2} $-(d^2q/(d\ln c \cdot dE) = 1.30*10^{-2}$ J m^{-2} V^{-2}		average $RT\,d'_c = 0.2970$ J m^2 C^{-2} $-(d^2E/(d\ln c \cdot dq) = 0.3230$ J m^2 C^{-2}	

the π-orbitals, as shown in Fig. 10c, consequently the C_β-hydrogens will prevent the tryptophan molecule from lying flat on the mercury surface thereby diminishing the intermolecular interaction between mercury and the tryptophan. In addition, the rotation about the C_α–C_β bond would be severely impeded or impossible.

In the case of tryptohan existing as a zwitter-ion, the resultant of the ion-pair dipole may be aligned with (Fig. 11a), or against (Fig. 11b), the dipole in the ring induced by the charge or field at the mercury surface. Even though the models may be imprecise, it can be seen that the most favourable condition for adsorption is when the mercury is positively charged: a zero charge density is a less-favourable condition, and a negative charge density a wholly unfavourable condition. If the zwitter-ion is oriented with the field, there will be some intramolecular repulsion on the solution side of the molecule, whereas if the orientation is against the field then intramolecular interaction should occur. It may well be that the lowest energy state will be one in which the ion-dipole moment is zero, Fig. 11c, as found by Baugh [28] for diglycine, and this would account for the low value of the coefficient of the linear term in Equation 11.

The plateau at high positive charge densities in the ϕ versus q curves, Fig. 6, is similar to that found by Hills [31] for p-aminobenzoic acid except that in their case, the plateau was found to be concentration-independent, i.e. all the curves were coincident in this region. From their data on the areas occupied by p-aminobenzoic acid, it was deduced that the molecule was adsorbed flat (horizontal) at high anodic charge densities, but vertical at the pzc where larger surface pressures were obtained. This suggestion is not considered to be valid for tryptophan for two reasons: first, saturation is not obtained at high anodic potentials and second, the suface area per molecule (discussed later) is larger than the minimum for the "flat" configuration, hence at the pzc, there is still sufficient room for the same configuration to be maintained. It seems reasonable that at high anodic potentials the zwitter-ion moiety may participate in the adsorption process by having its resultant dipole oriented with the field, and as the potential becomes less anodic, the dipole reorientates to give a zero moment, and this would account for the fact that, at cathodic potentials, the free energy becomes an almost-perfect parabolic function of potential.

Though tryptophan is adsorbed by displacing water molecules, maximum adsorption occurs not at the pzc but at anodic potentials because of π-electron interaction. The reason why the Esin and Markov coefficients are sensitive to changes in potential and charge in the cathodic regions is that small changes lead to progressively-more tilted strucures. In other words, at potentials more anodic than that of Γ^m, the molecule is lying flat on the mercury surface, π-electron interaction is strong, and rotation about the C_α–C_β bond is unimpeded: at potentials more cathodic than that of Γ^m, the molecule is progressively tilted, π-electron interaction diminishes, and rotation about the C_α–C_β bond is impeded. If this is the case, then cathodic and anodic coefficients of the various parameters will differ.

Of the adsorption isotherms considered, the Volmer isotherm has been shown to fit the data with E, and with q, as the control variable. The model of this isotherm is that of a non-localized monolayer, i.e. that any energy difference between sites of adsorption is less than kT, with the 'v' term giving an exclusion volume to allow for short-range repulsions between molecules. There is no term to account for longer-range repulsions between adsorbed molecules, and this is consistent with our model of adsorption of a neutral molecule and of a zwitter-ion with a freely-rotating dipole. The agreement between the isotherm parameter 'v' and the calculated area occupied by

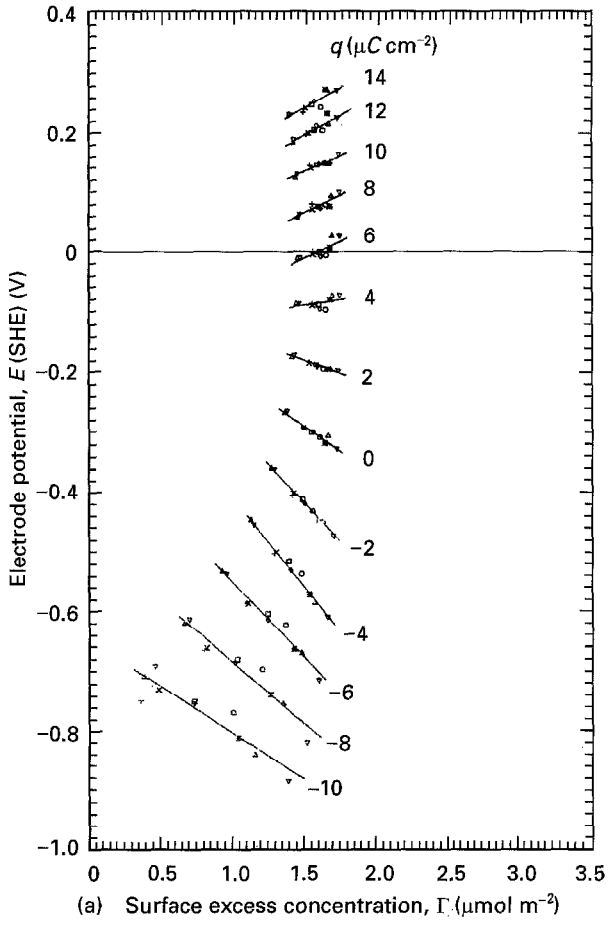

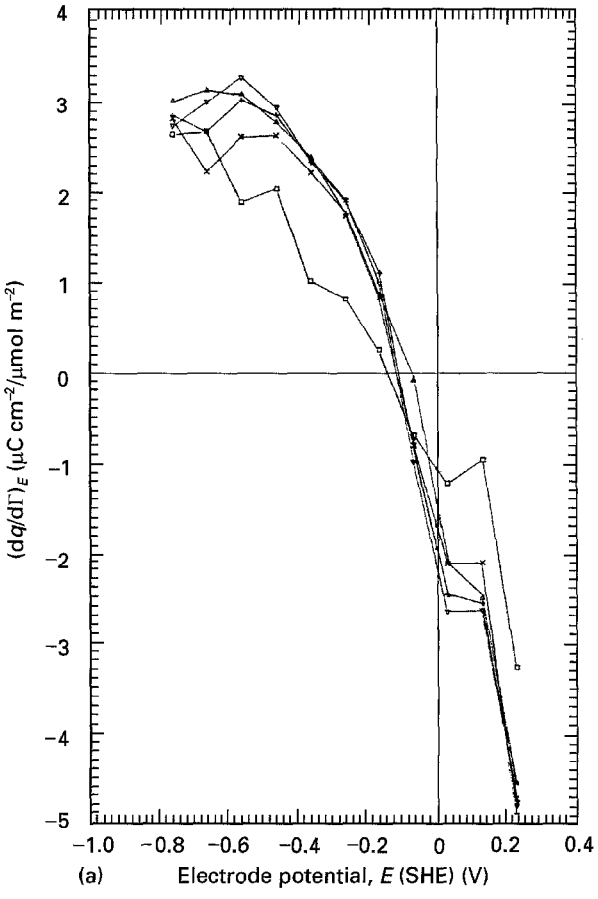

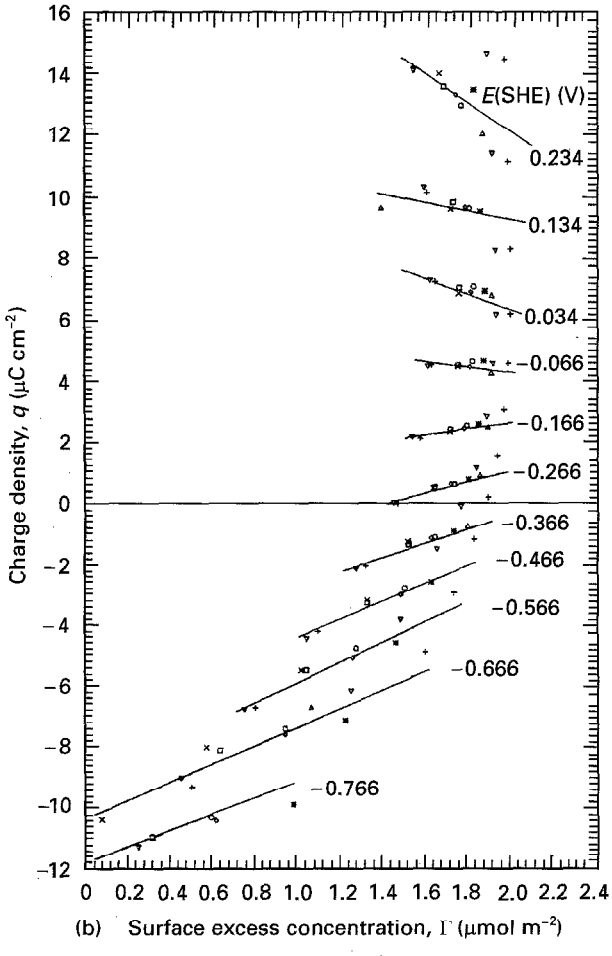

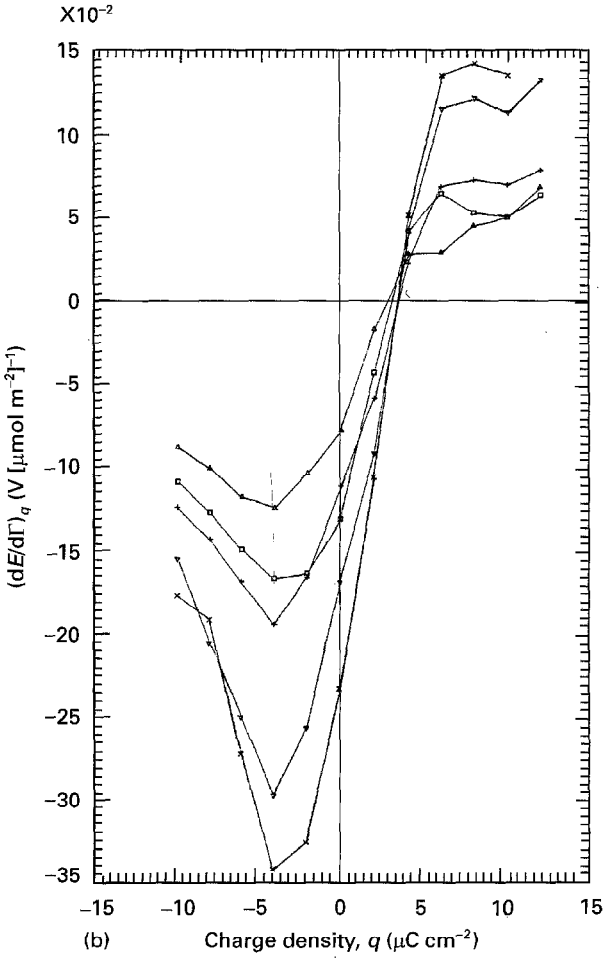

Figure 7 (a) Conway's "Esin and Markov" plots, electrode potential, E_q, versus surface excess concentration, $\Gamma(\pi)$, and (b) analogous plots of charge density, q_E, versus surface excess concentration, $\Gamma(\phi)$. Symbols as in Fig. 1.

Figure 8 (a) Coefficients (analogous to Conway's "Esin and Markov" coefficients) $(dq/d\Gamma(\phi))_E$, versus electrode potential E, and (b) $(dE/d\Gamma(\pi)_q$ versus charge density q. Symbols as in Fig. 3.

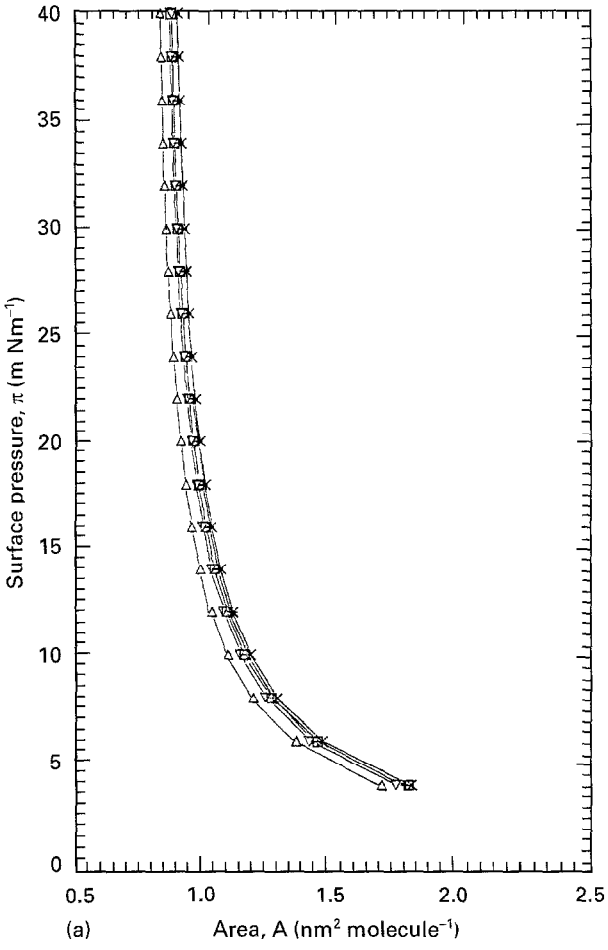

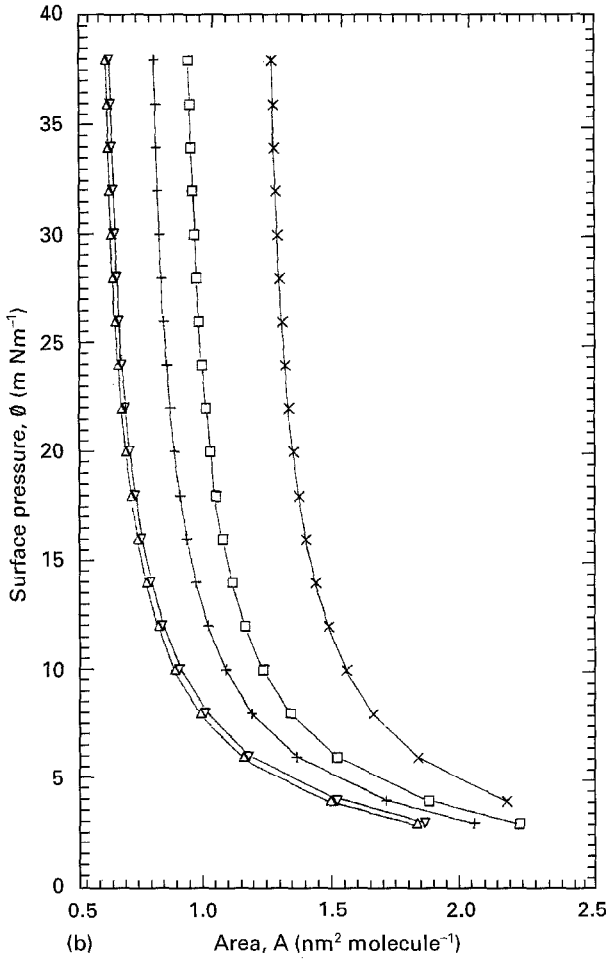

Figure 9 Surface pressures (a) π and (b) ϕ, versus area occupied, A, by an adsorbed tryptophan molecule. Symbols as in Fig. 3.

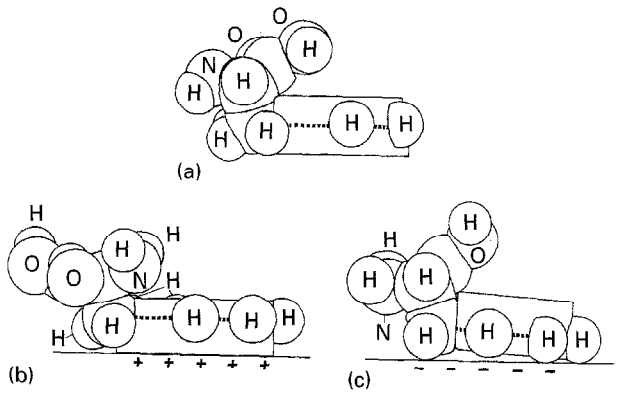

Figure 10 Catalin space models of an adsorbed non-ionized tryptophan molecule. See text for description.

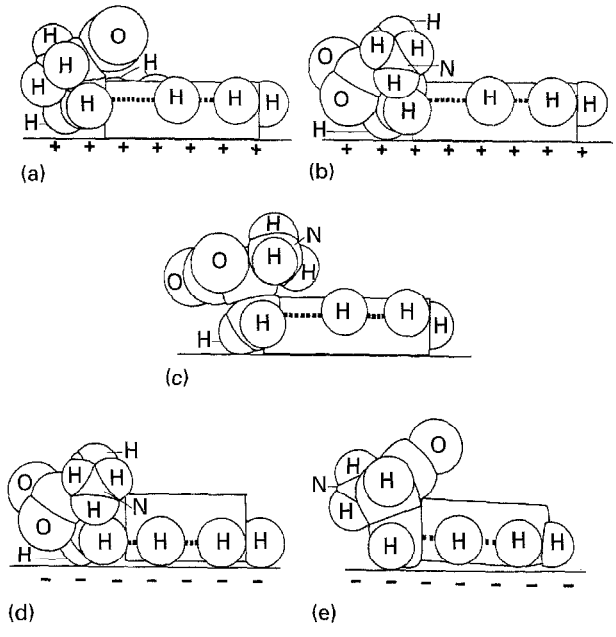

Figure 11 Catalin space models of an adsorbed zwitter-ionic tryptophan molecule. See text for description.

a tryptophan molecule lying flat, supports our interpretation. Various tests of congruence have been applied: the Volmer isotherm fits the experimental data for both electrical variables over a range of values, but the Esin and Markov, and Conway's 'Esin and Markov' coefficients show that congruence to either variable is not perfect .

The amino-acid group plays only a minor role in the adsorption process, and then only at high surface charge densities. This implies that the adsorption behaviour of a tryptophan fragment of a peptide or of blood and tissue proteins, would be similar. We therefore suggest that one reason why positively-charged (prostheses or electrode) surfaces are thrombogenic is that such surfaces are good adsorbents for dense π-electron systems such as tryptophan: even if the surfaces have zero charge density, they would still be strong adsorbents. It is only on surfaces of moderate-to-high negative charge densities that tryptophan would adopt a non-interactive mode. It is possible that adsorption of the tryptophan fragment of a blood protein would cause the protein to become distorted and hence be recognized an active centre for the next stage in

cascade thrombosis reaction. The electrostatic, and hence the electrokinetic, properties of any prosthesis plays a vital role in the initial stage of the blood, and tissue, interactive process, and this role should be considered seriously when prosthetic materials are being formulated.

Acknowledgement

This work was supported by the UK Engineering and Physical Sciences Research Council's programme on tissue-implant interactions, grant no. GR/B/0616.1.

References

1. F. MACRITCHIE, *Adv. Protein Chem.* **32** (1978) 283.
2. R. L. BEISSINGER and E. F. LEONARD, *Trans. Amer. Soc. Artif. Intern. Organs* **27** (1981) 225.
3. J. VERMIJLEN, M. VERSTRAETE and V. FUSTER, *J. Amer. Coll. Cardiol.* **8** (1986) 2B.
4. T. LINDHOUT, R. BLEZER, C. MAASSEN , V. HEINEN and C. M. P. REUTELINGSPERGER, *J. Mater. Sci. Mater. Med.* **6** (1995) 367.
5. L. DUIC, S. SRINIVASAN and P. N. SAWYER, *J. Electrochem. Soc.* **120** (1973) 348.
6. J. S. MATTSON and C. A. SMITH, *Science* **181** (1973) 1055.
7. H. L. MILLIGAN, J. DAVIS and K. W. EDMARK, *J. Biomed. Mater. Res.* **2** (1968) 51.
8. M. THUBIKAR, J. REICH and I. CADOFF, *J. Biomechanics* **13** (1980) 663.
9. M. COSTELLO, B. STANEZEWSKI, P. VRIESMAN, S. SRINIVASAN and P. N. SAWYER, *Trans. Amer. Soc. Artif. Int. Organs* **16** (1970) 1.
10. B. C. TAYLOR, W. V. SHARP, J. I. WRIGHT, K. L. EWING and C. L. WILSON, *ibid.* **17** (1971) 22.
11. J. B. CRAIG and C. MACKAY, *Talanta* **35** (1988) 365.
12. D. C. GRAHAME and R. B. WHITNEY, *J. Amer. Chem. Soc.* **64** (1941) 1548.
13. R. PARSONS and M. A. V. DEVANATHAN, *Trans. Farad. Soc.* **49** (1953) 404.
14. E. A. GUGGENHEIM and N. K. ADAM, *Proc. Roy. Soc. London A* **139** (1933) 218.
15. R. PARSONS, *Trans. Farad. Soc.* **51** (1955) 1518.
16. J. M. PARRY and R. PARSONS, *ibid.* **59** (1963) 241.
17. R. PARSONS, in "Reports 4th Soviet Conference on Electrochemistry, English Translation" (Consultants Bureau, New York, 1961), p 18.
18. *Idem., J. Electroanal. Chem.* **7** (1964) 136.
19. D. H. EVERETT, *Trans. Farad. Soc.* **46** (1950) 942.
20. R. PARSONS, *J. Electroanal. Chem.* **5** (1963) 397.
21. A. N. FRUMKIN, *Z. Phys. Chem.* 116 (1925) 466.
22. E. DUTKIEWITZ, J. D. GARNISH and R. PARSONS, *J. Electroanal. Chem.* **16** (1968) 505.
23. A. N. FRUMKIN, B. B. DAMASKIN and A. A. SURVILLA, *ibid.* **16** (1968) 93.
24. S. TRASATTI and G. J. OLIVIERI, *ibid.* **27** (1970) app 7.
25. A. de BATTISTI and S. TRASATTI , *ibid.* **48** (1973) 213.
26. J. A. V. BUTLER, *Proc. Roy. Soc. London* **A122** (1929) 399.
27. A. N. FRUMKIN, *Z. Phys.* **35** (1926) 792.
28. L. M. BAUGH and R. PARSONS, *Croatica Chem. Acta* **45** (1973) 127.
29. B. E. CONWAY and H. P. DHAR, *ibid.* **45** (1973) 109.
30. R. PARSONS, *Trans. Farad. Soc.* **55** (1959) 999.
31. G. J. HILLS, D. J. SCHIFFRIN and T. SOLOMON, *J. Electroanal. Chem. Interfacial Electrochem.* **41** (1973) 41.

Received 2 October
and accepted 17 November 1995